Robust Expansion Planning of Electric Vehicle Charging System and Distribution Networks

Yue Xiang, *Senior Member*, *IEEE*, Ping Xue, Yanliang Wang, Lixiong Xu, Wang Ma, Miadreza Shafie-khah, *Senior Member*, *IEEE*, Junlong Li, and Junyong Liu, *Member*, *IEEE*

***Abstract*—Large integration of electric vehicles (EVs) brings uncertainties and challenges for distribution networks. Reliability and allocation of charging systems (charging stations and piles) need strong support from the distribution network, whose expansion planning would be also greatly impacted by the incremental load from the charging system. To address this issue, a collaborative planning scheme of the EV charging system and distribution networks that combines economic and reliability benefits is proposed, which is formulated as a two-stage distributionally robust optimization model considering source-load uncertainties. First, a candidate EVCS planning scheme is obtained using queuing theory. Then, system reliability is quantified by adopting the average energy not supplied index and correlated integrated into the two-stage mixed-integer linear programming model. Finally, it is solved to perform distributionally robust expansion planning by the column and constraint generation algorithm. Effectiveness and scalability of the proposed planning method are illustrated by numerical case studies. Results indicate the planning scheme that considers economic and reliability benefit can perform better than traditional optimization methods.**

***Index Terms*—Distribution network planning, distributionally robust optimization, electric vehicle, reliability benefit.**

I. Introduction

THE high demand for energy conservation and pollution reduction must be satisfied under pressure of the environmental and energy crisis. According to statistics, carbon emissions in transportation account for approximately 30% of the total economic and social carbon emissions, and 75% of greenhouse gases and more than 90% of air pollutants are from activities in cities. Thus, energy saving and emission reduction in transportation are important to achieve the goal of "carbon peak and carbon neutrality". As clean and effective city transport means electric vehicles (EVs) are being vigorously developed. How to perform the planning of the EV charging system reasonably has become an important topic in satisfying growing charging demand. However, planning of the EV charging system and the planning of the distribution network interact with each other. Determination of the location and size of the EV charging station needs to consider grid's capacity while meeting transportation constraints. Meanwhile, the grid planning scheme also influences economy and reliability of the EV charging system. Hence, performing collaborative planning for the EV charging system and distribution network can meet charging and power load demand while optimizing coupled system operation. However, travel behavior of EV users entails subjectivity and randomness and is constrained by the operation of transportation and distribution networks. Large-scale integration of EVs into distribution networks brings operation risks and security challenges, particularly when high penetration of distributed generation (DG) exists in the grid. Therefore, we need to focus not only on the economic benefit when performing EV charging system and grid planning, but also on the reliability benefit of the planning scheme. A new type of power system is urgently constructed to perform adaptive planning for transportation and distribution networks in consideration of economic and reliability benefits.

EV charging behavior involves transportation and distribution networks. Thus, it is constrained by power flow and traffic flow. Multiple factors, such as charging demand satisfaction and grid adoption capacity, should be considered in the planning of the EV charging station (EVCS). In [1], a novel multiple-criteria decision-making method was proposed to determine an optimal EVCS site. In [2], allocation of administrative and residential EVCS was discussed based on a smart charging/discharging schedule to determine optimal capacity and location. Given characteristics of different types of private cars, an optimal EVCS planning scheme was proposed in [3] with minimum social cost of the overall EV charging system. However, these studies did not consider transportation constraints and ignored impacts of transportation network topology and traffic flow on EVCS planning. Dynamic interactions between evolution coherence of charging loads and traffic flows were captured in [4]. Reference [5] considered elastic traffic flow requirements, such as charging driving distance. However, the dynamic queuing process of EV users in the station was not considered.

In existing studies on the collaborative planning of EVCS

Manuscript received November 15, 2021; revised December 26, 2021, accepted March 1, 2022. Date of online publication December 30, 2022; date of current version March 27, 2023. This work was supported by the National Natural Science Foundation of China (52111530067), and the Academy of Finland project "Robust Distribution Network Planning to Facilitate Electric Vehicle Integration" (341473).

Y. Xiang, Y. L. Wang, L. X. Xu, W. Ma, J. Y. Liu are with College of Electrical Engineering, Sichuan University, Chengdu 610065, China.

P. Xue (corresponding author, email: xpsherry@foxmail.com) is with State Grid Sichuan Technical Training Center, Sichuan Electric Vocational and Technical College, and also the College of Electrical Engineering, Sichuan University, Chengdu 610065, China.

M. Shafie-khah is with the School of Technology and Innovations, University of Vaasa, Vaasa 8130, Finland.

J. L. Li is with the Department of Electronic and Electrical Engineering, University of Bath, Bath BA2 7AY, UK.

DOI: 10.17775/CSEEJPES.2021.08540

and distribution networks, the objective function usually involved maximizing economic benefit. However, they did not discuss whether the planning scheme could meet system operation requirements, particularly when multiple uncertain factors exist in the system. In [6], expansion planning of distribution network topology and EVCS was performed by minimizing investment and operation costs. A bi-level optimal allocation model for fast charging stations was proposed in [7]. The model coordinates investor benefit and user satisfaction degree. In consideration of the uncertainty of different types of charging load, a collaborative planning method for EVCS and distribution network was proposed in [8] to minimize investment and operation costs while maximizing captured traffic flow. However, the reliability benefit of the planning scheme was not considered in these studies. Reference [9] introduced a comprehensive evaluation index system to quantify the reliability level of distribution and transportation networks but did not present the planning scheme. In [10], reliability-correlated optimal planning of the distribution network and DG was proposed, but EV integration into the distribution network was ignored. In [11], a multi-objective optimal planning model was proposed. This model is oriented to collaborative improvement of distribution network operation reliability and EV travel reliability. Although reliability of the planning scheme was examined in [11], load curtailment was calculated based on system operation status, and failure rate was not considered. This scenario does not apply to actual operation and planning of the grid.

The main methods that describe uncertainty are stochastic optimization (SO) and robust optimization (RO) [12], [13]. In SO, characteristics of uncertain variables, such as wind power supply, are described using probability distribution, which has been applied early to power system planning [14], [15]. Reference [16] proposed a stochastic adaptive RO approach for generation and transmission expansion planning problems under a central planner perspective. Robust expansion planning of an electrical distribution system and EVCS was performed in [17]. Although SO and RO have already produced good results, SO requires support of a large number of scenarios, resulting in long calculation time, and RO needs to be utilized in the worst scenario, possibly leading to a conservative conclusion.

Given its good economic performance and conservativeness, distributionally robust optimization (DRO) has received much attention in the field of unit commitment and optimal scheduling. To address the uncertainty of DG power supply, a novel DRO approach was proposed in [18] to operate an energy hub system with an energy storage system. In [19], a distributionally robust chance-constrained generation expansion planning method was introduced considering long- and short-term uncertainties. This situation shows a few studies still utilize the DRO approach for collaborative planning of the EV charging system and distribution networks.

In summary, despite existing studies on collaborative planning of EVCS and distribution networks, the following limitations remain. (1) The reliability benefit, which is calculated based on failure rate information, has not been considered in planning research. (2) A few studies utilized the DRO approach for collaborative planning of EVCS and distribution networks, and did not evaluate impacts of uncertain factors on such planning.

To deal with these concerns, a two-stage distributionally robust collaborative planning model of the EV charging system and distribution network is proposed in consideration of economic and reliability benefits. The main contributions of this work are as follows:

- An optimal comprehensive target with balanced economic and reliability benefit is achieved for collaborative planning of EV charging system and distribution network. Compared with traditional method, the optimization model, which considers reliability benefit, can cope with uncertainties better while maintaining good operation benefit.
- A reliability benefit based on failure rate information is considered during the planning process. Thus, the obtained planning scheme is applicable to actual power grid operation.
- A DRO approach is utilized to deal with uncertainties of EV charging demand and DG output. Impact of uncertainties on collaborative planning of the distribution network and EV charging system is evaluated, and the corresponding optimal integrated penetration is provided.

The remainder of this paper is organized as follows: The framework of the study is introduced in Section II. Section III presents optimization of the EVCS planning scheme based on traffic flow. In Section IV, a proposed collaborative planning model of the distribution network and EV charging system is introduced together with a description of reliability benefit-based correlation analysis. The solving algorithm of the two-stage DRO model is presented in Section V. Effectiveness and scalability of the proposed planning method are tested in Section VI. Section VII concludes this work.

II. Research Framework

Given the uncertainties of charging load and wind output, a two-stage distributionally robust collaborative planning model of EVCS and a distribution network that considers the reliability benefit is proposed. The research framework is shown in Fig. 1.

As shown in Fig. 1, work in this paper is divided into three parts. For EVCS planning, it is optimized considering traffic flow based on queuing theory, which is planned from the perspective of people's behavior and psychological needs at the transportation network level. In this way, EVCS planning is decoupled with distribution network planning. Nevertheless, the obtained EVCS planning scheme is not the optimal solution since it still requires constraints from the distribution network. Hence, from this part, the candidate EVCS planning scheme is determined and is to be embedded into the collaborative planning model for optimal EVCS planning. For reliability benefit quantification part, the reliability benefit cannot be calculated directly with the expansion mixed-integer linear programming (MILP) planning model for its nonlinear characteristic. Thus, a correlation analysis method is used to quantify the reliability benefit. When the correlation rule has

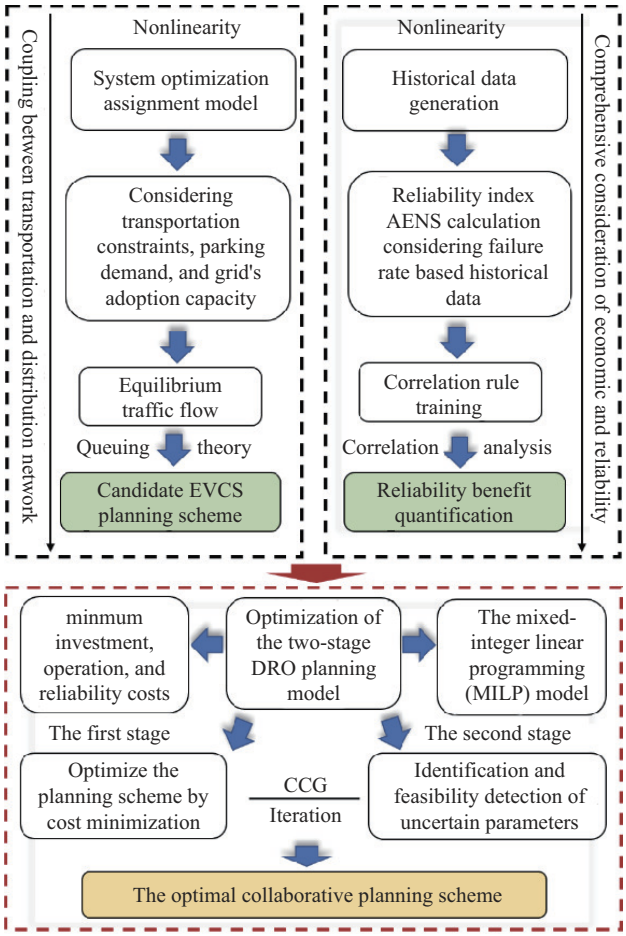

Fig. 1. Research framework.

been trained, it can be embedded into the MILP model, thereby improving calculation efficiency while ensuring its accuracy. With the obtained candidate EVCS planning scheme and the trained reliability correlation rule, a distributionally robust planning model can be simulated to determine the optimal collaborative planning scheme of EVCS and distribution network with a balanced economic and reliability benefit.

First, a candidate EVCS planning scheme is generated. A system optimization assignment (SOA) model, which focuses on EV users' charging behavior, is introduced to obtain equilibrium traffic flow in consideration of transportation constraints, parking demand, and grid's adoption capacity. Then, queuing theory is utilized to obtain a candidate EVCS configuration scheme. Second, the reliability calculation is linearized so it can be embedded into the mixed-integer linear programming (MILP) planning model. On this basis, the reliability index of average energy not supplied (AENS) is utilized to quantify system reliability. Third, reliability benefit calculation is embedded into the MILP model based on data obtained with the objective of achieving minimum investment and operation costs. Last, the collaborative planning scheme of the EV charging system and distribution network is optimized. An optimal collaborative planning scheme is obtained at the first stage with the objective of achieving minimum investment, operation, and reliability costs. An operational layer, which is used for identification and feasibility detection of uncertain parameters in the worst scenario, is considered at the second stage. A column and constraint generation algorithm is adopted to solve the MILP problem, which is linearized by big-M and second-order cone relaxation.

III. EVCS Optimization Based on Traffic Flow

A. Traffic Flow Assignment Model

Mobile EV charging demands at a specific traffic network node can be moderately reflected by traffic flow distribution. However, traffic flow and power flow data are generally dynamic and cannot be used directly during planning. Therefore, a typical operation scenario is considered in planning. Typical origin–destination (OD) data, which can be obtained from transportation departments or research results, characterize traffic flow distribution. On this basis, lowest travel cost is considered the objective function, and a SOA model is introduced to generate static traffic flow, which is expressed as:

$$\min \sum_{a\in N_T} fr_a t_a(fr_a) \tag{1}$$

$$\text{s.t.} \sum_k fp_k^{ru} = q_{ru} \quad fp_k^{ru} \geq 0 \tag{2}$$

$$fr_a = \sum_r \sum_u \sum_k fp_k^{ru} \delta_{a,k}^{ru} \tag{3}$$

$$t_a(fr_a) = t_a^0 \left[1 + b\left(\frac{fr_a}{c_a}\right)^v\right] \tag{4}$$

where fr_a represents traffic flow on road a. fp_k^{ru} is traffic flow of the OD matrix with regard to ru in path k. q_{ru} is total traffic flow with regard to ru. $\delta_{a,k}^{ru}$ is a 0–1 variable to indicate whether ru is included in path k or not. t_a represents the function of the Bureau of Public Roads. t_a^0 is travel time on road a. c_a is traffic capacity of road a, and b and v are retardation coefficients. Traffic flow based on the SOA model is defined as the "equilibrium traffic flow".

B. Candidate Number of EVCS Charger Determination and Charging Load Estimation

Charging demand is uncertain because of the randomness of EV users' charging behavior. The number of EVs arriving at the charging station can be obtained based on spatiotemporal traffic flow data. Given the transfer and aggregation characteristics of EVs, queuing theory is utilized to analyze EV charging behavior and determine the optimal configuration scheme of EVCS.

Users' charging behavior in the charging station can be characterized as a queuing system, where the EVCS charger provides charging service and EVs are customers. Assume the process of EVs arriving at the charging station obeys the Poisson distribution. In this case, when all EVCS chargers are in use, the first-come-first-served rule is followed. Others wait until an EVCS charger becomes available. Otherwise, users may choose to drive away if the waiting time exceeds their tolerance level. Charging service time obeys negative exponential distribution.

Parameter λ is the EV average arrival rate, i.e., the number of EVs reaching the charging station per unit time. It can be expressed as:

$$\lambda_{j,t} = \frac{H\omega\varepsilon_t fn_{j,t}}{\Delta t \sum_{j\in\Omega_T} fn_{j,t}} \tag{5}$$

where H is the total EV charging frequency on a typical day. w is the approximate ratio of charging frequency in the charging station to the total charging frequency. ε_t is the charging rate. $fn_{j,t}$ is traffic flow in the charging station located in bus j at time t, which can be accumulated by fr_a with the same injecting direction. Δt is the time step, and Ω_T represents the candidate set of charging station locations.

Indexes quantifying the station's charging service can be obtained as follows:

$$\rho = \frac{\lambda}{\mu} \tag{6}$$

$$\beta = \frac{\lambda}{s\mu} \tag{7}$$

$$\rho_0 = \frac{1}{\sum_{n=0}^{s-1} \frac{\rho^n}{n!} + \frac{\rho^s}{s!(1-\beta)}} \tag{8}$$

$$W_q = \frac{s\rho^{s+1}\rho_0}{\lambda s!(s-\rho)^2} \tag{9}$$

where μ is the EVCS chargers' service efficiency. ρ is average service rate of the charging system. β represents EVCS chargers' service rate. s is the number of chargers in the station. ρ_0 represents vacancy rate of the charging system, and W_q is average waiting time.

The number of chargers in an EVCS should be reduced as much as possible while still meeting users' charging demand to maximize return on investment. The minimum number of EVCS chargers can be calculated by considering users' average tolerance level of queuing time. The specific process is shown in Fig. 2.

In addition, distance between two charging stations should meet the geographical distance constraint.

$$d_{m-n} \geq d_{\min} \tag{10}$$

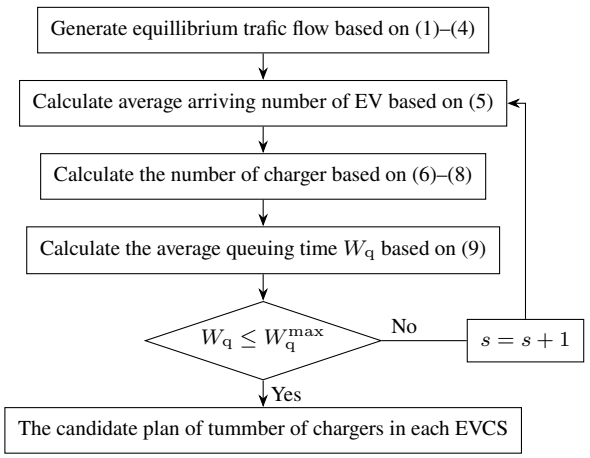

Fig. 2. Determination of the candidate charger number in each EVCS.

where d_{m-n} represents distance between bus m and n and $d_{\min}$ is the allowed shortest distance between charging stations.

Fast- and low-charging loads can be estimated after the candidate charging station configuration scheme is determined. Fast-charging load at time t can be estimated by combining EVCS charger's configuration results as follows:

$$\beta_{j,t}^{Cs} = \beta_{j,t} s_j P_{CD} \varpi, \tag{11}$$

where P_{CD} is power of the charger and ϖ is charging efficiency of the charger.

Meanwhile, slow-charging load is aggregated to the corresponding bus in the distribution network when a user charges an EV through a charging pile in a residential or commercial area. The number of charging piles in the node can be estimated with (12). On this basis, low-charging load can be calculated with (13).

$$N_i^{CP} = \frac{H \times (1-\omega) \times \sum_{t=1}^{T} P_{Li,t}}{\kappa \times (1-\gamma) \times \sum_{i=1}^{N_D} \sum_{t=1}^{T} P_{Li,t}} \tag{12}$$

$$P_{i,t}^{CP} = P_{CP} x_{i,t} N_i^{CP} \tag{13}$$

where κ represents charging capacity of the charging pile. $P_{Li,t}$ indicates active load in bus i at time t. γ is vacancy rate whose value is between 0 and 1. $x_{i,t}$ is charging demand coefficient, which can be represented by parking demand in a certain area, and P_{CP} is charging power of the charging pile.

IV. Collaborative Planning Model of the Distribution Network and EV Charging System

A. Objective Function

This study considers multi-objective planning with the highest economic and reliability benefits. Economic costs involve investment cost F^{inv}, operation cost F^{ope}, and reliability cost F^{rel}. Formulations are as follows:

$$\min \quad F^{\mathrm{inv}} + F^{\mathrm{ope}} + F^{\mathrm{rel}} \tag{14}$$

$$F^{\mathrm{inv}} = C_{\mathrm{sub}}^{\mathrm{inv}} + C_{\mathrm{line}}^{\mathrm{inv}} + C_{\mathrm{EVCS}}^{\mathrm{inv}} + C_{\mathrm{WTG}}^{\mathrm{inv}} + C_{\mathrm{chargingpile}}^{\mathrm{inv}} \tag{15}$$

$$F^{\mathrm{ope}} = \sum_{s=1}^{N_s} p_s \left(C_{\mathrm{sub}}^{\mathrm{ope}} + C_{\mathrm{WTGcur}}^{\mathrm{ope}} + C_{\mathrm{EVloadcur}}^{\mathrm{ope}} + C_{\mathrm{loss}}^{\mathrm{ope}}\right) + C_{\mathrm{line}}^{\mathrm{ope}} \tag{16}$$

$$C_{\mathrm{sub}}^{\mathrm{inv}} = \frac{r_0(1+r_0)^{m_{\mathrm{sub}}}}{r_0(1+r_0)^{m_{\mathrm{sub}}}-1} \left(\sum_{i\in\Psi_{\mathrm{subnewe}}} C^{\mathrm{sub\_new}} x_i^{\mathrm{sub\_new}} + \sum_{i\in\Psi_{\mathrm{subeex}}} C^{\mathrm{sub\_ext}} x_i^{\mathrm{sub\_ext}} \right) \tag{17}$$

$$C_{\mathrm{chargingpile}}^{\mathrm{inv}} = \frac{r_0(1+r_0)^{m_{\mathrm{pile}}}}{r_0(1+r_0)^{m_{\mathrm{pile}}}-1} \sum_{i\in\Psi_{\mathrm{pile}}} C^{\mathrm{pile}} x_i^{\mathrm{pile}} \tag{18}$$

$$C_{\mathrm{line}}^{\mathrm{inv}} = \frac{r_0(1+r_0)^{m_{\mathrm{L}}}}{r_0(1+r_0)^{m_{\mathrm{L}}}-1} \sum_{ij\in\Psi_{\mathrm{L}}} C^{\mathrm{L}} Len_{ij} x_{ij}^{\mathrm{L}} \tag{19}$$

$$C_{\mathrm{EVCS}}^{\mathrm{inv}} = \frac{r_0(1+r_0)^{m_{\mathrm{CS}}}}{r_0(1+r_0)^{m_{\mathrm{CS}}}-1} \sum_{i\in\Psi_{\mathrm{CS}}} x_i^{\mathrm{CS}} (C_i^{\mathrm{CS\_fix}} + s_i C_i^{\mathrm{CS\_var}}) \tag{20}$$

$$C_{\mathrm{WTG}}^{\mathrm{inv}}=\frac{r_0(1+r_0)^{m_{\mathrm{WTG}}}}{r_0(1+r_0)^{m_{\mathrm{WTG}}}-1}\sum_{i\in\Psi_{\mathrm{WTG}}}C^{\mathrm{WTG}}x_i^{\mathrm{WTG}} \tag{21}$$

$$C_{\mathrm{sub}}^{\mathrm{ope}}=D\delta^{\mathrm{sub}}\sum_{t\in T}\sum_{i\in\Psi_{\mathrm{sub}}}P_{s,i,t}^{\mathrm{sub}}x_i^{\mathrm{sub}} \tag{22}$$

$$C_{\mathrm{line}}^{\mathrm{ope}}=\delta^{\mathrm{L}}\sum_{ij\in\Psi_{\mathrm{L\_N}}}Len_{ij}\ \mathrm{L}_{ij}^{\mathrm{L\_N}} \tag{23}$$

$$C_{\mathrm{WTGcur}}^{\mathrm{ope}}=D\delta^{\mathrm{WTGcur}}\sum_{t\in T}\sum_{i\in\Psi_{\mathrm{WTG}}}(P_{s,i,t}^{\mathrm{WTG,Pre}}-P_{s,i,t}^{\mathrm{WTG}}) \tag{24}$$

$$C_{\mathrm{EVloadcur}}^{\mathrm{ope}}=D\delta^{\mathrm{EVloadcur}}\sum_{t\in T}\sum_{i\in\Psi_{\mathrm{pile}}}(P_{s,i,t}^{\mathrm{EVload,\ Pre}}-P_{s,i,t}^{\mathrm{EVload}}) \tag{25}$$

$$C_{\mathrm{loss}}^{\mathrm{ope}}=D\delta^{\mathrm{loss}}\sum_{t\in T}\sum_{ij\in\Psi_{\mathrm{L\_N}}}(I_{s,ij,t})^2r_{ij} \tag{26}$$

where i indicates a bus in the distribution network. t represents time. s represents scenario. N_s is number of scenarios. p_s represents probability of scenario occurrence. $C_{\mathrm{sub}}^{\mathrm{inv}}, C_{\mathrm{line}}^{\mathrm{inv}}$, $C_{\mathrm{EVCS}}^{\mathrm{inv}}, C_{\mathrm{WTG}}^{\mathrm{inv}}$, and $C_{\mathrm{chargingpile}}^{\mathrm{inv}}$ are investment costs of the substation, line, EVCS, WTG, and charging pile, respectively. $C_{\mathrm{sub}}^{\mathrm{ope}}$ and $C_{\mathrm{line}}^{\mathrm{ope}}$ are operation cost of the substation and line. $C_{\mathrm{WTGcur}}^{\mathrm{ope}}$ is wind curtailment cost. $C_{\mathrm{EVloadcur}}^{\mathrm{ope}}$ is EV charging load shedding cost. $C_{\mathrm{ops}}^{\mathrm{mec}}$ is cost of network loss. $m_{\mathrm{sub}}, m_{\mathrm{pile}}, m_{\mathrm{L}}$, m_{CS}, and m_{WTG} represent life cycle of the corresponding device. $C^{\mathrm{sub\_new}}$ and $C^{\mathrm{sub\_ext}}$ are new construction and expansion costs of the substation, respectively. C^{pile} is unit investment price of the charging pile. C^{L} is investment cost per unit length of the line. C^{WTG} is investment price for a single WTG. $x_i^{\mathrm{sub}}, x_i^{\mathrm{sub\_new}}, x_i^{\mathrm{sub\_ext}}, x_i^{\mathrm{pile}}, x_{ij}^{\mathrm{L}}, x_i^{\mathrm{CS}}$, and x_i^{WTG} are corresponding decision variables. Len_{ij} represents length of the line. s_i is charger number in the station. D is number of days in a year. δ^{sub} and δ^{L} are maintenance price. δ^{WTGcur} and $\delta^{\mathrm{EVloadcur}}$ are curtailment price of wind and charging load. δ^{loss} is network loss price. $P_{s,i,t}^{\mathrm{sub}}$ is output power of the substation. $P_{s,i,t}^{\mathrm{WTG,Pre}}, P_{s,i,t}^{\mathrm{WTG}}, P_{s,i,t}^{\mathrm{EVload,Pre}}$, and $P_{s,i,t}^{\mathrm{EVload}}$ are WTG forecasted output, WTG actual output, forecasted charging load, and actual charging load, respectively, and $\Psi_{\mathrm{sub}}, \Psi_{\mathrm{sub\_new}}, \Psi_{\mathrm{sub\_ext}}, \Psi_{\mathrm{pile}}, \Psi_{\mathrm{L}}, \Psi_{\mathrm{CS}}, \Psi_{\mathrm{wTG}}$, and $\Psi_{\mathrm{L\_N}}$ represent the set of corresponding devices' locating buses.

B. Constraints

1) Investment Constraint

$$0\le\sum_{y\in\Gamma^{\mathrm{sub}}}x_{i,y}^{\mathrm{sub}}\le 1 \tag{27}$$

$$\sum_{y\in\Gamma^{\mathrm{CS}}}x_{i,y}^{\mathrm{CS}}=1 \tag{28}$$

$$0\le x_i^{\mathrm{pile}}\le\overline{N}_i^{\mathrm{pile}} \tag{29}$$

$$0\le x_i^{\mathrm{WTG}}\le\overline{N}_i^{\mathrm{WTG}} \tag{30}$$

$$0\le\mathrm{Cap}^{\mathrm{WTG}}\sum_{i\in\Psi_{\mathrm{WTG}}}x_i^{\mathrm{WTG}}\le L^{\mathrm{WTG}}\sum_{i\in\Psi_{\mathrm{B\Omega}}}Load_i \tag{31}$$

where Γ^{sub} indicates whether substation is newly constructed or expanded. Γ^{CS} represents candidates of EVCS. $\Psi_{\mathrm{B\_N}}$ represents set of buses in the distribution network. $\overline{N}_i^{\mathrm{pile}}$ and $\overline{N}_i^{\mathrm{WTG}}$ represent maximum number of installed charging piles and WTGs. Cap^{WTG} is capacity of a single WTG. L^{WTG} is penetration limit of WTG in the grid, and $Load_i$ is load in bus i.

2) Branch Power Flow Constraint

Given the square of bus voltage and branch current is required in power flow equations, which are nonlinear, branch voltage and current should be transformed equivalently to linearize the planning model. $U_{s,i,t}^*$ and $I_{s,ij,t}^*$ are used to replace the square of the voltage and current as follows:

$$U_{s,i,t}^*=(U_{s,i,t})^2, \tag{32}$$

$$I_{s,ij,t}^*=(I_{s,ij,t})^2 \tag{33}$$

where $U_{s,i,t}^*$ and $I_{s,ij,t}^*$ are corresponding substitution variables.

With the big-M method [20], power flow equations can be expressed as:

$$\sum_{k\in\pi(i)}(P_{s,ki,t}-r_{ki}I_{s,ki,t}^*)-\sum_{j\in\varsigma(i)}P_{s,ki,t}+P_{s,i,t}^{\mathrm{sub}}+P_{s,i,t}^{\mathrm{WTG}}=P_{i,t}^{\mathrm{Load}}+P_{i,t}^{\mathrm{EVCS}}+P_{s,i,t}^{\mathrm{EVload}} \tag{34}$$

$$\sum_{k\in\pi(i)}(Q_{s,ki,t}-x_{ki}I_{s,ki,t}^*)-\sum_{j\in\varsigma(i)}P_{s,ki,t}+Q_{s,i,t}^{\mathrm{sub}}+Q_{s,i,t}^{\mathrm{WTG}}=Q_{i,t}^{\mathrm{Load}} \tag{35}$$

$$U_{s,j,t}^*\le U_{s,i,t}^*-2(r_{ij}P_{s,ij,t}+x_{ij}Q_{s,ij,t})+I_{s,ij,t}^*[(r_{ij})^2+(x_{ij})^2]+M(1-x_{ij}^{\mathrm{L}}) \tag{36}$$

$$U_{s,j,t}^*\ge U_{s,i,t}^*-2(r_{ij}P_{s,ij,t}+x_{ij}Q_{s,ij,t})+I_{s,ij,t}^*[(r_{ij})^2+(x_{ij})^2]-M(1-x_{ij}^{\mathrm{L}}) \tag{37}$$

$$I_{s,ij,t}^*U_{s,i,t}^*=(P_{s,ij,t})^2+(Q_{s,ij,t})^2 \tag{38}$$

Equation (38) can be transformed further as follows:

$$\left\|\begin{matrix}2P_{s,ij,t}\\2Q_{s,ij,t}\\I_{s,ij,t}^*-U_{s,i,t}^*\end{matrix}\right\|_2\le I_{s,ij,t}^*+U_{s,i,t}^* \tag{39}$$

where $\pi(i)$ and $\varsigma(i)$ are set of buses whose parent/child is bus i. r and x represent resistance and reactance, respectively, and P and Q represent active power and reactive power, respectively.

3) Security Constraint

$$(\underline{U})^2\le U_{s,i,t}^*\le(\overline{U})^2 \tag{40}$$

$$0\le I_{s,i,t}^*\le(\overline{I}_{ij})^2 \tag{41}$$

where $\underline{U}$ and $\overline{U}$ are the lower and upper limits of bus voltage, respectively, and $\overline{I_{ij}}$ is the upper limit of branch current.

4) Substation Injection Constraint

$$\underline{P}_i^{\mathrm{sub}}\le P_{s,i,t}^{\mathrm{sub}}\le\overline{P}_i^{\mathrm{sub}} \tag{42}$$

$$\underline{Q}_i^{\mathrm{sub}}\le Q_{s,i,t}^{\mathrm{sub}}\le\overline{Q}_i^{\mathrm{sub}} \tag{43}$$

where $\underline{P}_i^{\mathrm{sub}}$ and $\overline{P}_i^{\mathrm{sub}}$ are the lower and upper limits of substation injection power, respectively, the same applies to $\overline{Q}_i^{\mathrm{sub}}$ and $\underline{Q}_i^{\mathrm{sub}}$.

5) Branch Transmission Constraint

$$|P_{s,ij,t}| \le P_{ij}^{\max} \tag{44}$$

$$|Q_{s,ij,t}| \le Q_{ij}^{\max} \tag{45}$$

where $P_{ij}^{\max}$ and $Q_{ij}^{\max}$ are allowed maximum transmission power, respectively.

6) WTG Injection Constraint

$$0 \le P_{s,i,t}^{\mathrm{WTG}} \le P_{s,i,t}^{\mathrm{WTG,Pre}} \tag{46}$$

$$Q_{s,i,t}^{\mathrm{WTG}} = \tan[\cos^{-1}(\rho^{\mathrm{WTG}})] P_{s,i,t}^{\mathrm{WTG}} \tag{47}$$

where ρ^{WTG} is the power factor of WTG.

7) Uncertain Low-Charging Power Constraint

$$0 \le P_{s,i,t}^{\mathrm{EVload}} \le P_{s,i,t}^{\mathrm{EVload,Pre}} \tag{48}$$

8) Radial Operation Constraint

$$N_{\mathrm{L\_N}} = N_{\mathrm{B\_N}} - N_{\mathrm{sub}}(x_i^{\mathrm{sub}}) \tag{49}$$

where $N_{\mathrm{L\_N}}, N_{\mathrm{B\_N}}$, and N_{sub} are the number of lines, buses, and substations, respectively.

In addition, variable ε representing a small load is introduced to ensure the network's connection as follows:

$$\sum_{j\in\zeta(i)} P'_{s,ki,t} - \sum_{k\in\pi(i)} (P'_{s,ki,t} - r_{ki} I^{**}_{s,ki,t}) = \varepsilon \tag{50}$$

$$\sum_{j\in\zeta(i)} Q'_{s,ki,t} - \sum_{k\in\pi(i)} (Q'_{s,ki,t} - x_{ki} I^{*\prime}_{s,ki,t}) = \varepsilon \tag{51}$$

$$U^{*\prime}_{s,j,t} \le U^{*}_{s,i,t} - 2(r_{ij}P'_{s,j,t} + x_{ij}Q'_{s,j,s,}) + I^{*}_{s,ij,t}[(r_{ij})^2 + (x_{ij})^2] + M(1 - x^{\mathrm{L}}_{ij}) \tag{52}$$

$$U^{*\prime}_{s,j,t} \ge U^{*\prime}_{s,i,t} - 2(r_{ij}P'_{s,j,t} + x_{ij}Q'_{s,j,j}) + I^{*\prime}_{s,j,t}[(r_{ij})^2 + (x_{ij})^2] - M(1 - x^{\mathrm{L}}_{ij}) \tag{53}$$

$$\left\| \begin{matrix} 2P'_{s,ij,t} \\ 2Q^{s}_{s,ij,t} \\ I^{*}_{s,i,j,t} - U^{**}_{s,j,t} \end{matrix} \right\|_2 \le I^{*\cdot}_{s,j,t} + U^{*\prime}_{s,j,t}. \tag{54}$$

C. Correlation-based Reliability Benefit Calculation

Economic and reliability costs are considered when optimal investment planning is determined to ensure the planning scheme can maintain good effects. Reliability cost is calculated by considering load curtailment as follows:

$$F^{\mathrm{rel}} = \sigma \sum_{i\in\Psi_{\mathrm{S\_N}}} \mathit{AENS}_i \tag{55}$$

where σ is a penalty factor, $\Psi_{\mathrm{S\_N}}$ represents the network set, and AENS_i is the reliability index of AENS. Notably, (55) cannot be solved directly in a linear programming algorithm. Thus, a correlation analysis method is used to solve the multi-objective optimization problem, thereby improving calculation efficiency while ensuring calculation accuracy. Correlation analysis based on multiple linear regression can be expressed as follows:

$$\Phi_i(X, Y) = 0, \quad X \in R^{(x_i^{\mathrm{sub}}, x_{ij}^{L}, x_i^{\mathrm{pile}}, x_i^{\mathrm{CSs}}, x_i^{\mathrm{WTG}})} \tag{56}$$

where Φ_i indicates correlation analysis function, X is input data, including network topology and load, and Y is output data, namely, reliability index.

On the basis of data obtained, the correlation analysis is embedded into the linear programming model to improve calculation efficiency and accuracy. When historical data are trained, input is the uncertain variable set, namely, R in (56), and output is the reliability index. Numerous iteration calculations are needed during data training process. However, the optimization process in the linear programming calculation with the trained correlation rule is direct and efficient with no iteration. Then, the optimal planning scheme can be obtained.

V. Two-stage DRO Model and Solving Algorithm

A. DRO Model

Given the uncertainty of wind power and charging load, a two-stage collaborative planning model of the distribution network and EVCS is proposed. The first stage is the investment stage, which determines the investment plan of the substation, feeder, charging station, charging pile, and WTG. The second stage is for obtaining the worst scenario probability distribution with the objective of achieving minimum operation cost. The two-stage distributionally robust planning model can be expressed in the form of a matrix as follows:

$$\min_x Ax + \max_{p_s\in\Omega^P} \sum_{s=1}^{N_s} p_s \min_{y_s\in Y(x,\xi_s)} (By_s + K\xi_s) \tag{57}$$

$$Cx \le c \tag{58}$$

$$Dx = d \tag{59}$$

$$Ex + Fy_s = e \tag{60}$$

$$Gy_s \le g \tag{61}$$

$$\|Hy_s\|_2 \le h^{\mathrm{T}} y_s \tag{62}$$

$$Iy_s \le \xi_s \tag{63}$$

where x represents a discrete investment variable at the first stage, y indicates a continuous operation variable at the second stage, ξ represents forecasted wind power and charging load, and Ω^P is the set of scenarios. Eqs. (58) and (59) represent inequality and equation constraints at the first stage. Eq. (60) represents coupling of variables, such as power flow constraint, at the first and second stages. Eq. (61) represents the inequality constraint at the second stage, (62) represents the second-order cone constraints, and (63) represents the inequality constraints for uncertain variables and their forecasting value.

On the basis of the initial probability distribution of the typical scenario, norm-1 and nor-inf co-constraints are utilized to limit probability distribution fluctuation range. The confidence set can be expressed as follows:

$$\Omega^P = \left\{ \{p_s\} \left\{ \begin{matrix} p_s \ge 0, s = 1, \cdots, N_s \\ \sum_{s=1}^{N_s} p_s = 1 \\ \sum_{s=1}^{N_s} |p_s - p_s^0| \le \theta_1 \\ \max_{1\le s\le N_s} |p_s - p_s^0| \le \theta_\infty \end{matrix} \right. \right\} \tag{64}$$

where θ_1 and θ_∞ indicate the tolerance value of the norm-1 and norm-inf constraint. p_s satisfies the confidence level as follows:

$$P_r \left\{ \sum_{s}^{N_s} |p_s - p_s^0| \le \theta_1 \right\} \ge 1 - 2N_s e^{-2\mathrm{M}\theta_1/N_s} \tag{65}$$

$$P_r\left\{\max_{1\le s\le N_s}\left|p_s-p_s^0\right|\le\theta_\infty\right\}\ge 1-2N_s e^{-2M\theta_\infty} \tag{66}$$

The right-hand sides of (65) and (66) are set as α_1 and α_∞. Then, θ_1 and θ_∞ are obtained as follows:

$$\theta_1=\frac{N_s}{2L}\ln\frac{2N_s}{1-\alpha_1} \tag{67}$$

$$\theta_\infty=\frac{1}{2N_s}\ln\frac{2N_s}{1-\alpha_\infty} \tag{68}$$

where L is the amount of historical data.

B. Solving Algorithm

The two-stage distributionally robust model, shown in (57), can be divided into a master problem (MP) and a subproblem (SP), which can be solved based on a CCG algorithm. The model of MP is expressed as

$$\text{MP:}\quad \min_{x,y_s^m\in Y(x,\xi_s),W} Ax+W \tag{69}$$

$$\max_{p_s\in\Omega^P}\sum_{s=1}^{N_s}p_s^m\min_{y_s^m\in Y(x,\xi_s)}\left(By_s^m+K\xi_s\right),$$

$$\forall m=1,2,\cdots,M \tag{70}$$

$$\text{s.t.}\quad Cx\le c \tag{71}$$

$$Dx=d \tag{72}$$

$$Ex+Fy_s^m=e,\ \forall m=1,2,\cdots,M \tag{73}$$

$$Gy_s^m\le g,\ \forall m=1,2,\cdots,M \tag{74}$$

$$\left\|Hy_s^m\right\|_2\le h^{\mathrm{T}}y_s^m,\ \forall m=1,2,\cdots,M \tag{75}$$

$$Iy_s^m\le\xi_s,\ \forall m=1,2,\cdots,M, \tag{76}$$

where M is the number of iterations.

SP is optimized under the known investment plan. That is, after investment variables at the first stage are given, SP can be solved as follows:

$$\text{SP:}\quad f_{SP}(x^*)=\max_{p_s\in\Omega^P}\sum_{s=1}^{N_s}p_s^m\min_{y_s^m\in Y(x,\xi_s)}\left(By_s^m,K\xi_s\right)$$

$$\forall m=1,2,\cdots,M \tag{77}$$

The above-mentioned model can be solved by dividing it into two layers. Confidence set Ω^P is not associated with constraints of the variable at the second stage. Consequently, the minimum problem in the inner layer is solved first. Then, the maximum problem to obtain the worst probability distribution is optimized. The solving process has been presented by [21].

VI. Case Studies

A. Input Data

A modified 54-node distribution network and the Sioux–Falls transportation network are used in this study as the test system. Four substations with three existing substations are considered. Substations 51, 52, and 53 have initial capacities of 5, 10, and 2 MW, respectively; among them, substations 52 and 53 consider expanding. One candidate substation (substation 54) to be constructed is also considered. Moreover, five charging stations in 11 candidate locations, 17 candidate feeders, and 15 candidate WTG locations are considered. The unit installation capacity and maximum installation number of WTG are 0.25 MW and 40, respectively. Prices of network loss, power generation, and wind curtailment are set with reference to [21] and [22]. Value of the penalty factor σ is set to 250 to comprehensively consider economic and reliability benefits of the planning scheme. When σ is set to 250, the benefits of economy and reliability can be well balanced, reflecting characteristics of the planning scheme that considers reliability while maintaining its economy. Low- and fast-charging powers are 10 and 60 kW, respectively. The OD matrix on a typical day can be seen in [23]. Forecasting scenario of low-charging load and WTG output are shown in Figs. 3 and 4. Other parameters, including topology of transportation and distribution network and corresponding coupling information, candidate substation planning schemes, some basic investment and operation parameters, and traffic data, are given in https://docs.qq.com/pdf/DR2ZUZUFTZkNBWm9B.

B. Analysis of The EVCS Planning Scheme

According to the traffic flow assignment model proposed in this study, 19 possible EVCS configuration schemes are obtained, including EVCS planning location and number of chargers in the station.

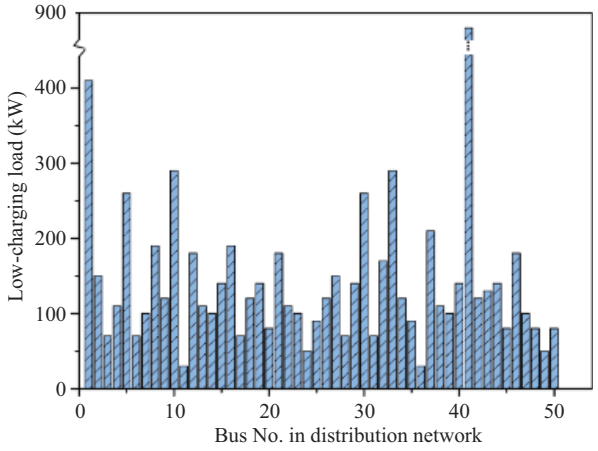

Fig. 3. Low-charging load forecast.

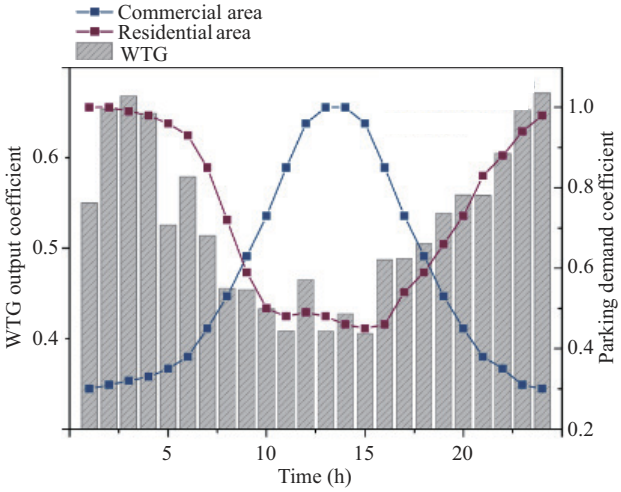

Fig. 4. WTG output forecast.

TABLE I
CANDIDATE PLANNING SCHEMES OF EVCS

Schemes	Bus in the Distribution Network										
	6	26	33	31	30	13	15	27	28	47	14
1	7	10	0	9	0	7	0	0	0	8	0
2	7	9	0	9	0	7	0	0	0	0	9
3	7	9	0	9	0	0	0	0	0	8	9
4	7	10	0	0	9	7	0	0	0	8	0
5	7	10	0	0	9	7	0	0	0	0	9
6	7	9	0	0	9	0	0	0	0	8	9
7	7	10	0	0	0	7	0	0	0	8	9
8	7	0	0	9	0	6	0	10	0	0	9
9	7	0	0	9	0	7	0	0	0	8	10
10	7	0	0	9	0	0	0	10	0	8	9
11	7	0	0	0	9	6	0	10	0	0	9
12	7	0	0	0	9	7	0	0	0	8	10
13	7	0	0	0	8	0	0	10	0	8	9
14	0	9	0	9	0	6	0	0	0	8	9
15	0	9	0	0	9	6	0	0	0	8	9
16	0	0	0	9	0	6	0	10	0	8	9
17	0	0	0	8	0	0	0	9	10	7	8
18	0	0	0	0	8	6	0	10	0	8	9
19	0	0	0	0	7	0	0	9	10	7	8

Nineteen EVCS-optimized schemes meet charging demand based on traffic flow. Corresponding fast-charging load can be estimated according to the planning scheme. For example, for Schemes 1 and 19, estimated fast-charging load is shown in Fig. 5. Fast-charging load within 1 day basically shows a normal distribution because the EVCSs are all located in a business district where the charging peak is concentrated from 12:00 to 15:00. EVCS candidates are applied to the distribution network optimization problem, and the planning results are shown in the next part.

C. Contrastive Analysis Based on Different Cases

According to Part B, 19 possible EVCS configuration schemes are obtained and analyzed. On this basis, a total of 10,000 scenarios are generated by stochastic simulation to represent the uncertainty of the WTG output and EV charging load. Then, the K-means clustering method is used to obtain four typical scenarios. The following cases are defined to verify effectiveness of the proposed planning method.

Case 1: Optimal planning based on the deterministic optimization method ignoring reliability benefit.

Case 2: Optimal planning based on DRO method ignoring reliability benefit.

Case 3: Optimal planning based on the deterministic optimization method considering reliability benefit.

Case 4: Optimal planning based on DRO method considering reliability benefit.

As shown in Table II, a contrastive analysis based on Case 1 and Case 2 is performed, where the planning results differ based on the two different optimization methods. Comparison of Case 1 and Case 2 indicate the feeder changes from line 54–22 to line 22–23 by applying the DRO method. A probable reason is the distance of line 54–22 is short, resulting in low investment and maintenance costs; meanwhile, substation 51 has enough backup to undertake the load increase. The uncertainty is considered using DRO. Thus, compared with the traditional method, the DRO method exhibits a growth trend in planning of WTG and charging piles. WTG locations with increased investment installation, such as buses 25, 39, and 27, are all distributed at the end of the transmission line. Thus, compared with upgrading the substation, expanding the WTG installation can increase efficiency if the load is increased at the end of the line. In addition, Fig. 6 indicates the investments on charging piles increase when the DRO method is utilized, particularly for bus 41. The reason is that low-charging load is estimated based on corresponding power load. The power load is inherently large for bus 41. Therefore, charging piles at bus 41 increase after considering the uncertainty.

Tables II and III show the charging load curtailment, generation, and total operation costs using the DRO method are lower than those using traditional deterministic optimization method. This finding indicates planning results based on DRO can effectively ensure a reliable power supply and good economic benefit while coping with uncertain scenarios.

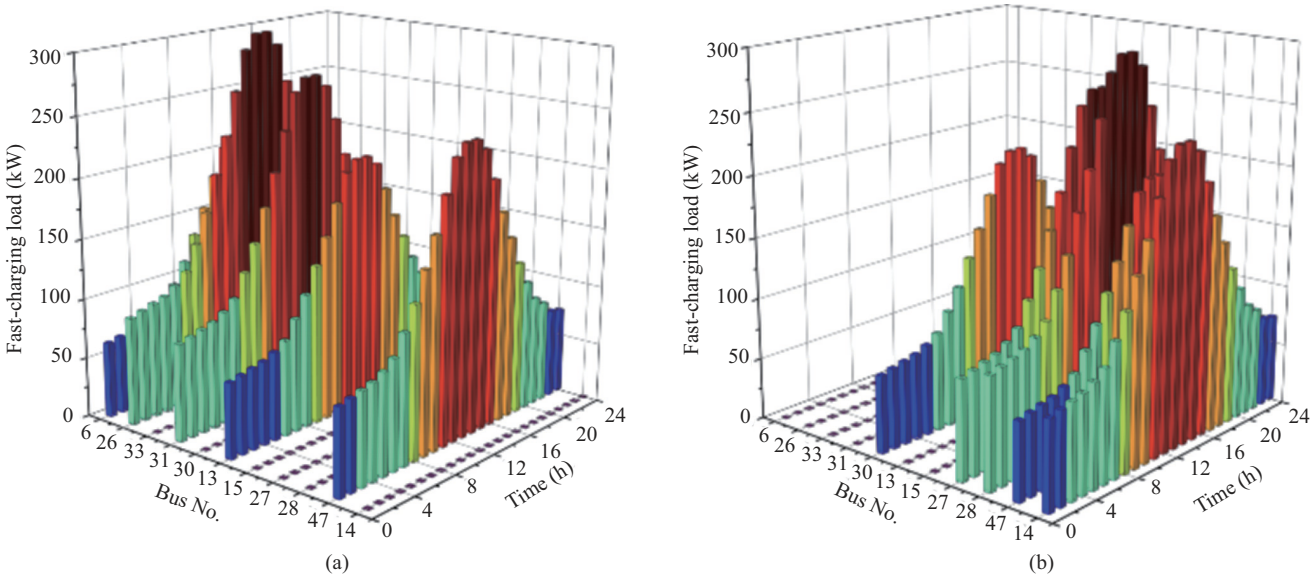

Fig. 5. Fast-charging load estimation with certain EVCS schemes. (a) Scheme 1. (b) Scheme 19.

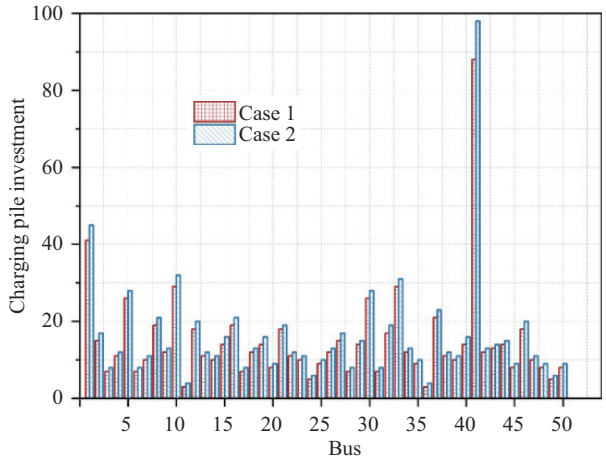

Fig. 6. Planning results of the charging pile based on deterministic optimization and DRO methods.

TABLE II
PLANNING RESULTS BASED ON DETERMINISTIC OPTIMIZATION AND DRO METHODS IGNORING RELIABILITY BENEFIT

	Investment Scheme						Cost
	Sub	Line		EVCS	WTG		($\times 10^8$ yuan)
Case 1	52(0,0)	54–21	41–42	Scheme 4	20(12)	42(0)	2.0003
	53(0,1)	54–22	42–48		25(4)	6(0)	
	54(0,1,0)	54–30	48–49		39(8)	26(6)	
		30–29	49–50		16(14)	31(13)	
		53–41	37–31		50(5)	30(6)	
					13(12)	27(4)	
					28(0)	47(4)	
					14(0)		
Case 2	52(0,0)	22–23	41–42	Scheme 4	20(11)	42(0)	1.9714
	53(0,1)	54–21	42–48		25(9)	6(0)	
	54(0,1,0)	54–30	48–49		39(9)	26(6)	
		30–29	49–50		16(14)	31(13)	
		53–41	37–31		50(5)	30(0)	
					13(12)	27(5)	
					28(0)	47(4)	
					14(0)		

TABLE III
COSTS BASED ON DETERMINISTIC OPTIMIZATION AND DRO METHODS IGNORING RELIABILITY BENEFIT

	Costs/($\times 10^8$ yuan)					
	Investment	Line Operation	Generation	Network Loss	Wind Curtailment	EV Charging Load Curtailment
Case 1	0.4401	0.0060	1.5209	0.0178	0	0.0155
Case 2	0.4393	0.0059	1.4996	0.0181	0	0.0085

Presence of the reliability benefit is considered when making a decision, and comparative results are shown in Tables IV and V. Planning results of the charging piles are similar to the results above. Thus, these results are not listed here.

Table IV indicates that network topology changes from line 41–42 to line 42–47 after considering the reliability benefit. The reason is that line 42–47 has a section switch, which can reduce response time and restore power supply quickly when a shortage occurs. Moreover, the expanding scheme for substation 53 changes from Scheme b to Scheme a, because of its power supply pressure due to change of network topology. Therefore, substation 52 must be upgraded to ensure a reliable power supply for the new increase in load.

TABLE IV
PLANNING RESULTS BASED ON DETERMINISTIC OPTIMIZATION AND DRO METHODS CONSIDERING THE RELIABILITY BENEFIT

	Investment Scheme						Cost
	Sub	Line		EVCS	WTG		($\times 10^8$ yuan)
Case 3	52(1,0)	54–21	42–47	Scheme 4	20(11)	42(6)	2.7389
	53(1,0)	54–22	42–48		25(3)	6(0)	
	54(0,1,0)	54–30	48–49		39(30)	26(6)	
		30–29	49–50		16(5)	31(11)	
		53–41	37–31		50(6)	30(6)	
					13(0)	27(4)	
					28(0)	47(0)	
					14(0)		
Case 4	52(1,0)	54–21	42–47	Scheme 4	20(11)	42(0)	2.7110
	53(1,0)	54–22	42–48		25(9)	6(0)	
	54(0,1,0)	54–30	48–49		39(9)	26(6)	
		30–29	49–50		16(14)	31(13)	
		53–41	37–31		50(5)	30(0)	
					13(12)	27(5)	
					28(0)	47(4)	
					14(0)		

In addition, the WTG investment planning results based on deterministic optimization method have changed greatly after reliability benefits are considered. The reason is that planning schemes based on deterministic optimization method can only respond to a specific scenario, and maintaining them to be stable when the environment changes is difficult. By contrast, investment planning based on DRO highly tends to withstand fluctuation of the outside environment, thereby confirming effectiveness of the proposed method.

Table V shows the operation benefit from deterministic optimization and DRO methods after considering the reliability benefit. System reliability is mainly related to network topology. Thus, reliability costs in Table V are identical. When the reliability benefit is considered, system operation cost, including generation, network loss, charging load, and shedding costs, decreases. In particular, the EV load curtailment cost decreases by nearly 50%. This finding indicates the operation benefit is improved after considering the reliability benefit.

TABLE V
COSTS BASED DETERMINISTIC OPTIMIZATION AND DRO METHOD CONSIDERING THE RELIABILITY BENEFIT

	Costs/($\times 10^8$ yuan)						
	Reliability	Investment	Line Operation	Generation	Network loss	Wind Curtailment	EV Charging Load Curtailment
Case 3	0.7283	0.4572	0.0059	1.5200	0.0162	0	0.0113
Case 4	0.7283	0.4582	0.0059	1.4980	0.0159	0	0.0047

D. Contrastive Analysis Based on Different EV Penetrations

Figure 7 shows planning results on different EV penetrations. Extent of substation expansion increases as EV penetration increases from 0.1 to 0.3. For network topology, topology based on a method that ignores the reliability benefit also changes with increase in EV penetration; when the reliability benefit is considered, the topology changes only after EV penetration exceeds 20%. This scenario indicates the method proposed in this study, i.e., the method that considers the reliability benefit, can cope with load increments and ensure the effectiveness of planning better than the traditional method

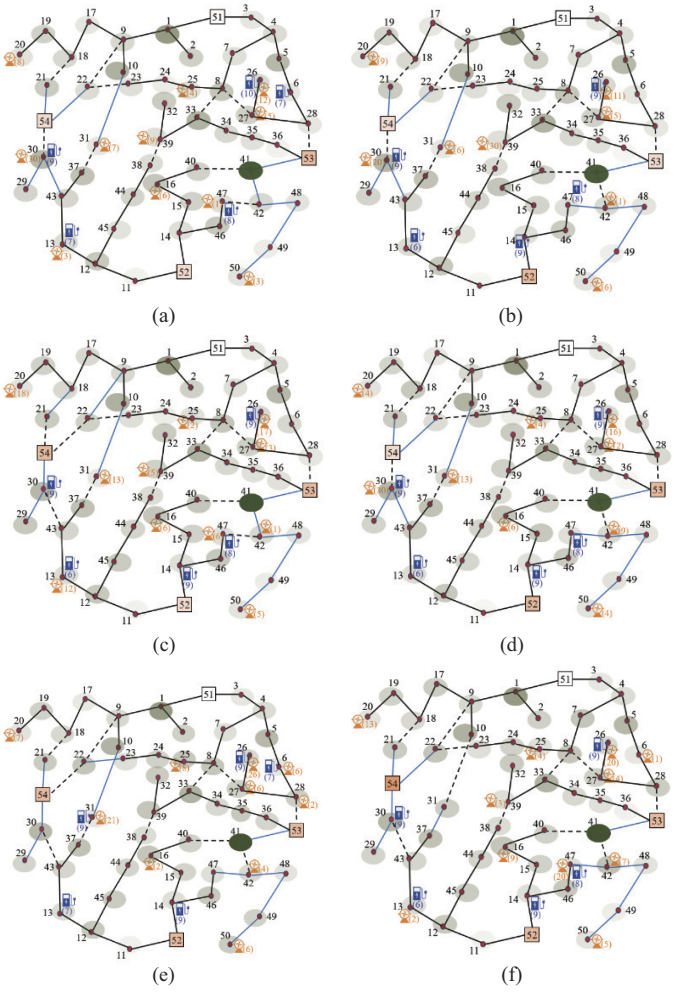

Fig. 7. Planning results based on different EV penetrations. (a) 0.1 is set as EV penetration ignoring reliability benefit. (b) 0.1 is set as EV penetration considering reliability benefit. (c) 0.2 is set as EV penetration ignoring reliability benefit. (d) 0.2 is set as EV penetration considering reliability benefit. (e) 0.3 is set as EV penetration ignoring reliability benefit. (f) 0.3 is set as EV penetration considering reliability benefit.

can (i.e., the method without considering the reliability benefit of the planning scheme). With the increase in EV penetration, the EVCS planning scheme based on the traditional method changes from Scheme 4 to Scheme 5 and finally to Scheme 2, thereby increasing cost. With a method that considers the reliability benefit, the planning scheme of EVCS is maintained at Scheme 15. This finding further proves that EVCS planning based on the proposed method can accommodate charging load increments while maintaining good economic benefit. The total costs of WTG investment are identical because the penetration limit of WTG is fixed. However, distribution of WTG installation differs to adapt to change in network topology and load increase. Investment on the charging pile also increases correspondingly.

Figure 8 shows total planning cost change with increase in EV penetration. Planning cost considering the reliability benefit is higher than one based on the traditional method. However, the growth rate of the cost based on the traditional method is higher than one considering the reliability benefit. Moreover, the relative increase rate of Cost A to Cost B is downward. These findings further explain that investment planning considering the reliability benefit is more suitable for a power system with multi-energy integration and fast-growing load than investment planning based on the traditional method.

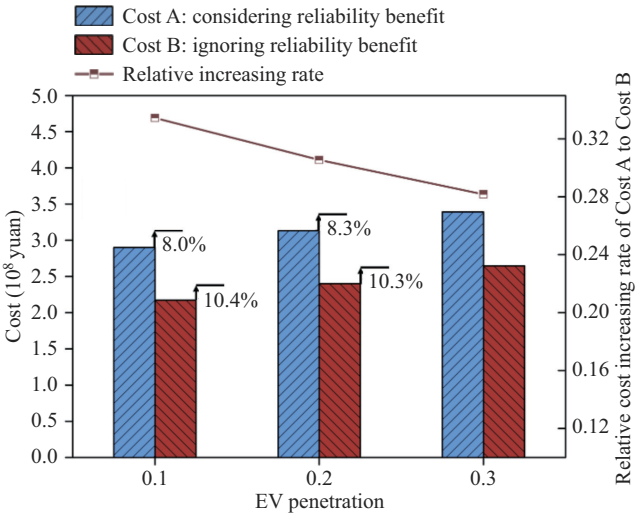

Fig. 8. Cost of planning schemes based on different EV penetrations.

E. Contrastive Analysis Based on Different DG Penetrations

Changes in network topology and WTG investment are analyzed in this section by considering DG integration in the grid. For a planning scheme that considers the reliability benefit, network topology remains unchanged until WTG penetration exceeds 50%. However, for a planning scheme based on the traditional method, network topology changes with the increase in WTG penetration, further verifying the applicability and effectiveness of the method proposed in this study. Fig. 9 presents changes in network topology under different WTG penetrations. Fig. 10 shows a comparison of WTG planning schemes based on different WTG penetrations.

Bus 31 and 33 are incorporated into substation 51 from other power supply regions when DG penetration is increased from 0.5 to 0.6. Hence, WTG investment in this area is increased, particularly for bus 25, which is located close to the new load point. With the traditional method, only substations 51 and 52 remain when WTG penetration is 60%. Although the substation investment is reduced, topology at this time cannot resist environmental changes and cannot guarantee system operation reliability, particularly when large-scale renewable energy is integrated into the distribution network. Costs of the planning schemes are shown in Table VI. Total cost decreases as operation cost decreases. However, reliability and investment costs start to increase when DG penetration exceeds 50%. With reference to the previous analysis of network topology, the optimal DG penetration is presumably 50% at the current load level.

F. Contrastive Analysis Based on DRO and RO Approach

To analysis performance of DRO approach used in this paper, a robust optimization method is adopted to perform the contrastive simulation. Range of uncertain variables in RO is

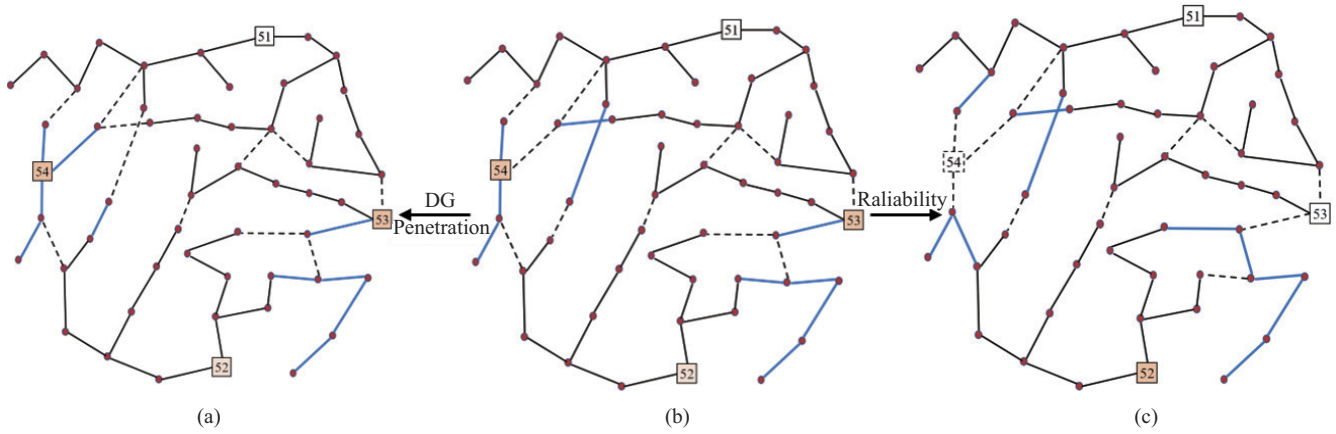

Fig. 9. Planning results of network topology based on different conditions. (a) WTG penetration = 0.5 considering the reliability benefit. (b) WTG penetration = 0.6 considering the reliability benefit. (c) WTG penetration = 0.6 ignoring the reliability benefit.

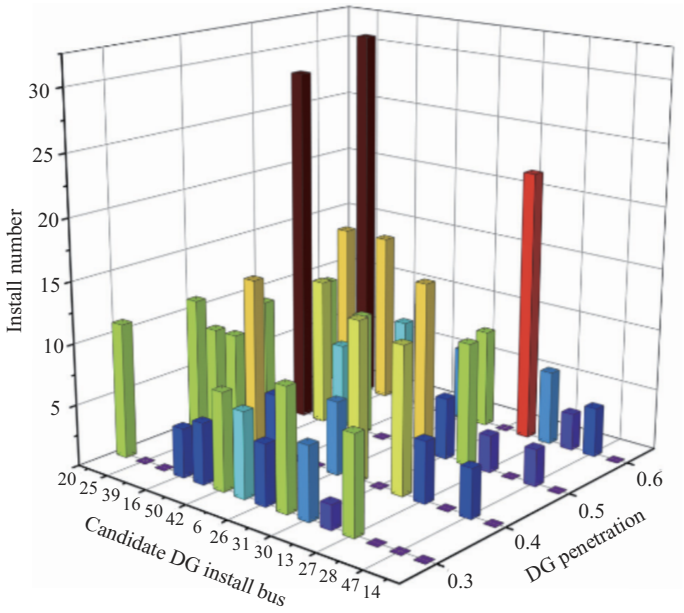

Fig. 10. WTG planning results based on different WTG penetrations.

TABLE VI
COSTS OF PLANNING SCHEMES BASED ON DIFFERENT WTG PENETRATIONS

WTG Penetration	Objective Function ($\times 10^8$ yuan)			
	Reliability Cost	Investment Cost	Operation Cost	Total
0.3	0.7283	0.4642	1.6735	2.8677
0.4	0.7283	0.4577	1.5245	2.7122
0.5	0.7283	0.4362	1.426	2.5922
0.6	0.7508	0.4812	1.2452	2.4772

0.2 times the predicted value. The following cases are defined to do performance analysis.

Case 5: Optimal planning based on RO approach ignoring reliability benefit.

Case 6: Optimal planning based on RO approach considering reliability benefit.

Planning results based on Case 5 and Case 6 are shown in Tables VII and VIII. Comparing Case 5 and Case 2, which can be seen from Tables VII and II, it can be found that network topology is changed. Applying the obtained distribution planning result to perform simulation operation, the result is given the reliability level of distribution network based Case 5 is greater than Case 2 ($F^{\text{rel}}_{\text{Case 5}}$ is 0.7559 and $F^{\text{rel}}_{\text{Case 2}}$ is 0.7691). However, investment and operation cost of planning scheme based Case 5 is larger than Case 2, while the reliability level of Case 2 is also within an acceptable range. It shows compared to RO method, DRO method achieves good balance in economy and conservativeness. For Case 6 and Case 4, which is shown in Table VIII, planning results have no significant difference. This is because after considering reliability benefit during planning process, the investment scheme can cope with uncertainties better, which also verifies effectiveness of the proposed method in this paper. Nonetheless, a cost based RO approach is still larger than DRO method. This also

TABLE VII
PLANNING RESULTS BASED ON RO METHOD IGNORING RELIABILITY BENEFIT

	Investment Scheme						Cost ($\times 10^8$ yuan)
	Sub	Line		EVCS	WTG		
Case 5	52(0,0)	10–31	53–41	Scheme 4	20(6)	42(0)	2.0769
	53(0,1)	54–21	41–42		25(1)	6(0)	
	54(0,1,0)	54–22	42–48		39(7)	26(8)	
		54–30	48–49		16(15)	31(6)	
		30–29	49–50		50(3)	30(5)	
					13(25)	27(3)	
					28(0)	47(8)	
					14(1)		

TABLE VIII
PLANNING RESULTS BASED ON RO METHOD CONSIDERING RELIABILITY BENEFIT

	Investment Scheme						Cost ($\times 10^8$ yuan)
	Sub	Line		EVCS	WTG		
Case 6	52(1,0)	54–21	42–47	Scheme 4	20(9)	42(6)	2.8020
	53(1,0)	54–22	42–48		25(3)	6(0)	
	54(0,1,0)	54–30	48–49		39(31)	26(8)	
		30–29	49–50		16(5)	31(10)	
		53–41	37–31		50(6)	30(5)	
					13(0)	27(5)	
					28(0)	47(0)	
					14(0)		

confirms the good economy of DRO method.

Specific cost analysis is conducted in Tables IX and X. It can be seen that network operation cost based on RO method is larger than DRO method whether or not the reliability benefit is considered. This is because for RO method, it is operated in the worst scenario. For DRO approach, it can ensure a degree of reliable grid operation while maintaining good economy. In general, when performing the collaborative planning of EVCS and distribution network, planning results based on DRO approach can achieve good balance in economy and conservativeness.

TABLE IX
COSTS BASED ON DRO AND RO METHOD IGNORING RELIABILITY BENEFIT

Case	Costs ($\times 10^8$ yuan)					
	Investment	Line Operation	Generation	Network Loss	Wind Curtailment	EV Charging Load Curtailment
2	0.4393	0.0059	1.4996	0.0181	0	0.0085
5	0.4413	0.0060	1.5896	0.0215	0	0.0185

TABLE X
COSTS BASED ON DRO AND RO METHOD CONSIDERING THE RELIABILITY BENEFIT

Case	Costs ($\times 10^8$ yuan)						
	Reliability	Investment	Line Operation	Generation	Network loss	Wind Curtailment	EV Charging Load Curtailment
4	0.7283	0.4582	0.0059	1.4980	0.0159	0	0.0047
6	0.7283	0.4576	0.0059	1.5851	0.0169	0	0.0082

VII. CONCLUSION

Given the uncertainty of charging load and wind power output, a two-stage distributionally robust collaborative planning model of the EV charging system and distribution network, which considers the reliability benefit, is proposed in this study. The following conclusions are drawn from the case studies.

1) Compared with a traditional method, an optimization model that considers the reliability benefit can cope with uncertainties better while maintaining good operation benefit. Operation costs, such as network loss cost, decrease at different levels, particularly EV load curtailment cost, which decreases by nearly 50%.

2) Distribution network planning results in topology obtained with the traditional method, which ignores the reliability benefit, and change with increase in EV penetration. However, with the proposed method that considers the reliability benefit, the topology changes only after EV penetration exceeds 20%.

3) Optimal DG penetration is 50% when network topology and investment and operation costs are considered comprehensively. When DG penetration exceeds 50%, network topology must be replanned, and reliability and investment costs increase.

4) Compared with the deterministic optimization method, the DRO method considers real-time uncertainty of renewable energy and charging load, thereby simulating the distribution network with multi-energy integration effectively. Planning results based on DRO method can also achieve good balance in economy and conservativeness, which helps power system planners make a suitable grid expansion scheme.

REFERENCES

[1] H. C. Liu, M. Y. Yang, M. C. Zhou, and G. D. Tian, "An integrated multi-criteria decision making approach to location planning of electric vehicle charging stations," *IEEE Transactions on Intelligent Transportation Systems*, vol. 20, no. 1, pp. 362–373, Jan. 2019.

[2] E. Hadian, H. Akbari, M. Farzinfar, and S. Saeed, "Optimal allocation of electric vehicle charging stations with adopted smart charging/discharging schedule," *IEEE Access*, vol. 8, pp. 196908–196919, Oct. 2020.

[3] H. C. Zhang, Z. C. Hu, Z. W. Xu, and Y. H. Song, "An integrated planning framework for different types of PEV charging facilities in urban area," *IEEE Transactions on Smart Grid*, vol. 7, no. 5, pp. 2273–2284, Sep. 2016.

[4] Y. Xiang, Z. P. Liu, J. C. Liu, Y. B. Liu, and C. H. Gu, "Integrated traffic-power simulation framework for electric vehicle charging stations based on cellular automaton," *Journal of Modern Power Systems and Clean Energy*, vol. 6, no. 4, pp. 816–820, Feb. 2018.

[5] X. Y. Gan, H. X. Zhang, G. Hang, Z. D. Qin, and H. M. Jin, "Fast-charging station deployment considering elastic demand," *IEEE Transactions on Transportation Electrification*, vol. 6, no. 1, pp. 158–169, Mar. 2020.

[6] X. Wang, M. Shahidehpour, C. W. Jiang, and Z. Y. Li, "Coordinated planning strategy for electric vehicle charging stations and coupled traffic-electric networks," *IEEE Transactions on Power Systems*, vol. 34, no. 1, pp. 268–279, Jan. 2019.

[7] Y. B. Liu, Y. Xiang, Y. Y. Tan, B. Wang, J. Y. Liu, and Z. Y. Yang, "Optimal allocation model for EV charging stations coordinating investor and user benefits," *IEEE Access*, vol. 6, pp. 36039–36049, Jun. 2018.

[8] S. Wang, Z. Y. Dong, F. J. Luo, K. Meng, and Y. X. Zhang, "Stochastic collaborative planning of electric vehicle charging stations and power distribution system," *IEEE Transactions on Industrial Informatics*, vol. 14, no. 1, pp. 321–331, Jan. 2018.

[9] P. Xue, Y. Xiang, J. Gou, W. T. Xu, W. Sun, Z. Z. Jiang, S. Jawad, H. J. Zhao, and J. Y. Liu, "Impact of large-scale mobile electric vehicle charging in smart grids: a reliability perspective," *Frontiers in Energy Research*, vol. 9, pp. 688034, Jun. 2021.

[10] Y. Xiang, Y. Wang, Y. C. Su, W. Sun, Y. Huang, and J. Y. Liu, "Reliability correlated optimal planning of distribution network with distributed generation," *Electric Power Systems Research*, vol. 186, pp. 106391, Sep. 2020.

[11] Y. Xiang, J. P. Meng, D. Huo, L. X. Xu, Y. F. Mu, C. H. Gu, K. Kou, and F. Teng, "Reliability-oriented optimal planning of charging stations in electricity–transportation coupled networks," *IET Renewable Power Generation*, vol. 14, no. 18, pp. 3690–3698, Dec. 2020.

[12] H. M. A. Ahmed, A. B. Eltantawy, and M. M. A. Salama, "A planning approach for the network configuration of AC-DC hybrid distribution systems," *IEEE Transactions on Smart Grid*, vol. 9, no. 3, pp. 2203–2213, May 2018.

[13] N. Amjady, A. Attarha, S. Dehghan, and A. J. Conejo, "Adaptive robust expansion planning for a distribution network with DERs," *IEEE Transactions on Power Systems*, vol. 33, no. 2, pp. 1698–1715, Mar. 2018.

[14] J. H. Roh, M. Shahidehpour, and L. Wu, "Market-based generation and transmission planning with uncertainties," *IEEE Transactions on Power Systems*, vol. 24, no. 3, pp. 1587–1598, Aug. 2009.

[15] L. Baringo and A. J. Conejo, "Correlated wind-power production and electric load scenarios for investment decisions," *Applied Energy*, vol. 101, pp. 475–482, Jan. 2013.

[16] L. Baringo and A. Baringo, "A stochastic adaptive robust optimization approach for the generation and transmission expansion planning," *IEEE Transactions on Power Systems*, vol. 33, no. 1, pp. 792–802, Jan. 2018.

[17] N. B. Arias, A. Tabares, J. F. Franco, M. Lavorato, and R. Romero, "Robust joint expansion planning of electrical distribution systems and EV charging stations," *IEEE Transactions on Sustainable Energy*, vol. 9, no. 2, pp. 884–894, Apr. 2018.

[18] P. F. Zhao, C. H. Gu, D. Huo, Y. C. Shen, and I. Hernando-Gil, "Two-stage distributionally robust optimization for energy hub systems," *IEEE Transactions on Industrial Informatics*, vol. 16, no. 5, pp. 3460–3469, May 2020.

[19] F. Pourahmadi, J. Kazempour, C. Ordoudis, P. Pinson, and S. H. Hosseini, "Distributionally robust chance-constrained generation expansion planning," *IEEE Transactions on Power Systems*, vol. 35, no. 4, pp. 2888–2903, Jul. 2020.
[20] S. F. Kong, Z. J. Hu, S. W. Xie, L. Yang, and Y. F. Zheng, "Two-stage robust planning model and its solution algorithm of active distribution network containing electric vehicle charging stations," *Transactions of China Electrotechnical Society*, vol. 35, no. 5, pp. 1093–1105, Mar. 2020.
[21] S. J. He, H. J. Gao, J. Y. Liu, Y. B. Liu, J. Y. Wang, and Y. Xiang, "Distributionally robust optimal DG allocation model considering flexible adjustment of demand response," *Proceedings of the CSEE*, vol. 39, no. 8, pp. 2253–2264, Apr. 2019.
[22] H. J. Gao and J. Y. Liu, "Coordinated planning considering different types of DG and load in active distribution network," *Proceedings of the CSEE*, vol. 36, no. 18, pp. 4911–4922, Sep. 2016.
[23] L. J. LeBlanc, E. K. Morlok, and W. P. Pierskalla. (2021, Sep.). Sioux-Falls network. [Online]. Available: http://www.bgu.ac.il/~bargera/tntp/.

Yue Xiang received the B.S. and Ph.D. degrees from Sichuan University, China, in 2010 and 2016, respectively. From 2013 to 2014, he was a joint Ph.D. student at the Department of Electrical Engineering and Computer Science, University of Tennessee, Knoxville, US and also a visiting scholar at the Department of Electronic and Electrical Engineering, University of Bath, UK in 2015. Currently, he is a Professor at the College of Electrical Engineering, Sichuan University, China. His main research interests are electric vehicles, power system planning and optimal operations, renewable energy integration and smart grids.

Ping Xue received the B.S. and M.S. degrees from Sichuan University, China, in 2019 and 2022, respectively. Currently, she is working at State Grid Sichuan Technical Training Center, and also the Sichuan Electric Vocational and Technical College. Her main research interests are electric vehicles, distribution network planning and optimal operations.

Yanliang Wang received the B.Eng. degree from Chengdu University of Technology, China, in 2021. He received the M.S. degree in Electrical Engineering, Sichuan University, China, in 2024. His research focuses on electric vehicles.

Lixiong Xu received the B.S., M.S., and Ph.D. degrees from Sichuan University, Chengdu, China, in 2003, 2006, and 2014, respectively. He is currently an Associate Professor in Power System with the College of Electric Engineering, Sichuan University. His research interests include AI in smart grids, power system security and stability.

Wang Ma received the B.S. and M.S. degrees in Electrical Engineering from Sichuan University, Chengdu, China, in 2019 and 2022, respectively. Her research interests include distribution network operation and dynamic reconfiguration.

Miadreza Shafie-khah received his first Ph.D. in Electrical Engineering from Tarbiat Modares University, Tehran, Iran. He received his second Ph.D. in Electromechanical Engineering and first postdoc from the University of Beira Interior (UBI), Covilha, Portugal. He received his second postdoc from the University of Salerno, Salerno, Italy. Currently, he is a Professor at the University of Vaasa, Vaasa, Finland. He is an Editor of the IEEE Transactions on Sustainable Energy, an Associate Editor of the IEEE Systems Journal, an Associate Editor of the IEEE Access, an editor of the IEEE Open Access Journal of Power and Energy (OAJPE), an Associate Editor for IET-RPG, the guest Editor-in-Chief of the IEEE OAJPE, the guest editor of IEEE Transactions on Cloud Computing, and the guest editor of more than 14 Special Issues. He was considered one of the Outstanding Reviewers of the IEEE Transactions on Sustainable Energy, in 2014 and 2017, one of the Best Reviewers of the IEEE Transactions on Smart Grid, in 2016 and 2017, and one of the Outstanding Reviewers of the IEEE Transactions on Power Systems, in 2017 and 2018, and one of the Outstanding Reviewers of IEEE OAJPE, in 2020. He has co-authored more than 420 papers that received more than 10000 citations with an h-index equal to 55. He is also the volume editor of the book "Blockchain-based Smart Grids", Elsevier, 2020. He is a Top Scientist in the Guide2Research Ranking in computer science and electronics, and he has won five Best Paper Awards at IEEE Conferences. His research interests include power market simulation, market power monitoring, power system optimization, demand response, electric vehicles, price and renewable forecasting and smart grids.

Junlong Li received the B.Eng. degree in College of Electrical Engineering from Sichuan University, Chengdu, China, in 2015 and 2019. He received the Ph.D. degree in Electronic and Electrical Engineering at the University of Bath, in 2023. His main research interests include edge-cloud computing in power systems and energy management system.

Junyong Liu received his Ph.D. degree from Brunel University, UK, in 1998. He is a Professor in the college of Electrical Engineering, Sichuan University, China. His main research interests are power system planning, operation, stability and computer applications.